

# The ALK inhibitor ASP3026 eradicates NPM-ALK<sup>+</sup> T-cell anaplastic large-cell lymphoma *in vitro* and in a systemic xenograft lymphoma model

Suraj Konnath George<sup>1,\*</sup>, Deeksha Vishwamitra<sup>1,2,\*</sup>, Roxsan Manshoury<sup>1,2</sup>, Ping Shi<sup>3</sup> and Hesham M. Amin<sup>1,2</sup>

<sup>1</sup> Department of Hematopathology, The University of Texas M. D. Anderson Cancer Center, Houston, TX

<sup>2</sup> The University of Texas Graduate School of Biomedical Sciences, Houston, TX

<sup>3</sup> State Key Laboratory of Bioreactor Engineering, East China University of Science and Technology, Shanghai, China

\* These authors contributed equally to this work

Correspondence to: Hesham M. Amin, email: hamin@mdanderson.org

Keywords: NPM-ALK, ASP3026, T-cell lymphoma, crizotinib, CHOP

Received: June 22, 2014

Accepted: July 4, 2014

Published: July 5, 2014

This is an open-access article distributed under the terms of the Creative Commons Attribution License, which permits unrestricted use, distribution, and reproduction in any medium, provided the original author and source are credited.

## ABSTRACT

**NPM-ALK<sup>+</sup> T-cell anaplastic large-cell lymphoma (ALCL) is an aggressive type of cancer. Standard treatment of NPM-ALK<sup>+</sup> ALCL is CHOP polychemotherapy. Although patients initially respond favorably to CHOP, resistance, relapse, and death frequently occur. Recently, selective targeting of ALK has emerged as an alternative therapeutic strategy. ASP3026 is a second-generation ALK inhibitor that can overcome crizotinib resistance in non-small cell lung cancer, and is currently being evaluated in clinical trials of patients with ALK<sup>+</sup> solid tumors. However, NPM-ALK<sup>+</sup> ALCL patients are not included in these trials. We studied the effects of ASP3026 on NPM-ALK<sup>+</sup> ALCL cell lines *in vitro* and on systemic lymphoma growth *in vivo*. ASP3026 decreased the viability, proliferation, and colony formation, as well as induced apoptotic cell death of NPM-ALK<sup>+</sup> ALCL cells. In addition, ASP3026 significantly reduced the proliferation of 293T cells transfected with NPM-ALK mutants that are resistant to crizotinib and downregulated tyrosine phosphorylation of these mutants. Moreover, ASP3026 abrogated systemic NPM-ALK<sup>+</sup> ALCL growth in mice. Importantly, the survival of ASP3026-treated mice was superior to that of control and CHOP-treated mice. Our data suggest that ASP3026 is an effective treatment for NPM-ALK<sup>+</sup> ALCL, and support the enrollment of patients with this lymphoma in the ongoing clinical trials.**

## INTRODUCTION

Anaplastic lymphoma kinase (ALK) is a receptor tyrosine kinase that is expressed in neuronal cells at an early stage of human development; therefore, it is assumed that ALK contributes to neural tissue development [1, 2]. In addition to its physiologic expression, ALK is aberrantly expressed in several human cancers, including an aggressive subtype of T-cell lymphoma known as ALK-expressing anaplastic large-cell lymphoma (ALK<sup>+</sup> ALCL) [3]. The expression of ALK in this lymphoma occurs secondary to one of several chromosomal aberrations that involve the *ALK* gene on chromosome 2p23. The most common of these aberrations is translocation t(2;5)

(p23;q35) that occurs in 85% of ALK<sup>+</sup> ALCL cases [3, 4]. This translocation also involves the nucleophosmin (*NPM*) gene and induces the generation of the oncogenic tyrosine kinase NPM-ALK.

NPM is a ubiquitously expressed protein that shuttles ribonucleoproteins between the nucleolus and cytoplasm. Unlike ALK, NPM-ALK lacks an extracellular domain. Nonetheless, NPM-ALK appears to be constitutively activated by the formation of the NPM-ALK/NPM-ALK homodimers through the NPM domain. Wild-type NPM is also involved in the formation of NPM/NPM-ALK heterodimers that translocate to the nucleus [5]. Because NPM-ALK is the most widely expressed ALK chimeric protein and because all established ALK<sup>+</sup>

T-cell ALCL cell lines harbor NPM-ALK, in this paper we will refer to this lymphoma as NPM-ALK<sup>+</sup> ALCL.

Although NPM-ALK<sup>+</sup> ALCL represents only 3-5% of non-Hodgkin lymphomas in adults, it constitutes up to 40% of these lymphomas in children and adolescents. NPM-ALK<sup>+</sup> ALCL is an aggressive cancer; most patients present with advanced stage (III/IV) disease, widespread dissemination, and B symptoms including high fever, night sweats, and weight loss [3]. There is no specific therapeutic approach for NPM-ALK<sup>+</sup> ALCL, and it is typically treated with doxorubicin-containing polychemotherapy such as CHOP (cyclophosphamide, doxorubicin, vincristine, and prednisone). A few studies have systematically analyzed the outcomes of therapeutic approaches for NPM-ALK<sup>+</sup> ALCL, and, not unexpectedly, most of these studies focused on pediatric patients [6-13]. Patients usually show an initial favorable response to CHOP; however, 30-40% of the patients in these studies had multiple relapses and disease/therapy-associated death remains a common event [7, 12].

Because ALK plays crucial roles in the development and survival of NPM-ALK<sup>+</sup> ALCL [14], targeting ALK is viewed as a promising strategy for treating NPM-ALK<sup>+</sup> ALCL patients [15]. Although selective ALK inhibitors are being evaluated in clinical trials, most of these trials focus on ALK<sup>+</sup> solid tumors such as non-small cell lung cancer (NSCLC), neuroblastoma, and inflammatory myofibroblastic tumor [16-18].

ASP3026 (2-N-[2-methoxy-4-[4-(4-methylpiperazin-1-yl)piperidin-1-yl]phenyl]-4-N-(2-propan-2-ylsulfonylphenyl)-1,3,5-triazine-2,4-diamine) is a recently developed, orally available, second-generation small molecule ALK inhibitor. ASP3026 was identified in an ALK inhibition assay aimed at the oncogenic fusion kinase echinoderm-microtubule-associated protein-like 4-ALK (EML4-ALK) that has been detected in a subgroup of NSCLC patients [19, 20]. Initial studies showed that ASP3026 possesses remarkable inhibitory effects on EML4-ALK activity. Preliminary studies in NSCLC showed that compared with crizotinib (PF-02341066, Xalkori), an ALK/c-MET/ROS1 inhibitor that has been approved to treat patients with relapsed ALK<sup>+</sup> NSCLC, ASP3026 is more tolerable and more potent in inhibiting EML4-ALK [20]. Importantly, crizotinib-resistant EML4-ALK mutants were not resistant to the effects of ASP3026 [20-23].

Because of these encouraging results, ASP3026 is currently being evaluated in clinical trials (<http://clinicaltrials.gov/show/NCT01401504>; <http://clinicaltrials.gov/ct2/show/NCT01284192>) that enroll patients with aggressive ALK<sup>+</sup> solid tumors and ALK<sup>+</sup> large B-cell lymphoma, which, compared with NPM-ALK<sup>+</sup> T-cell ALCL, is a very rare entity with less than 40 patients reported [24]. A preliminary analysis concluded that ASP3026 possesses promising safety and pharmacokinetic profiles [25]. Although NPM-ALK<sup>+</sup> ALCL was the first

type of cancer in which ALK was identified, the effects of ASP3026 have not been evaluated in this neoplasm. More importantly, NPM-ALK<sup>+</sup> ALCL patients are not eligible for enrollment in the ongoing trials.

Herein, we sought to perform a systematic *in vitro* analysis of the effects of ASP3026 on NPM-ALK<sup>+</sup> ALCL cells. In addition, we developed and utilized a systemic xenograft NPM-ALK<sup>+</sup> ALCL model in SCID mice to examine the effects of this inhibitor *in vivo*. Our data provide strong evidence that ASP3026 is an efficacious treatment for the aggressive NPM-ALK<sup>+</sup> ALCL, and support the inclusion of NPM-ALK<sup>+</sup> ALCL patients in the ongoing clinical trials.

## RESULTS

### ASP3026 decreases NPM-ALK<sup>+</sup> ALCL cell viability

At 48 h, ASP3026 induced concentration-dependent decreases in the viability of all NPM-ALK<sup>+</sup> ALCL cell lines tested, as measured by MTS assay (Fig. 1A). DEL cells, particularly at lower concentrations of 0.1, 0.5, and 1.0  $\mu$ M, demonstrated less sensitivity to ASP3026 than the other cell lines. The IC<sub>50</sub> was 0.4  $\mu$ M in SU-DHL-1, 0.75 in SUP-M2, 1.0 in SR-786, 2.5 in Karpas 299, and > 3.0 in DEL cell lines. Similar effects were not observed in the T lymphocytes that were used as a negative control and the decrease in the viability of the lymphoma cells was significantly greater than the decrease in the viability of the T lymphocytes. The decrease in cell viability became more pronounced at 72 h, and the IC<sub>50</sub> was 0.3  $\mu$ M in SU-DHL-1, 0.5 in DEL, 0.75 in SUP-M2 and SR-786, and 2.5 in Karpas 299 (Fig. 1B).

### ASP3026 induces apoptosis in NPM-ALK<sup>+</sup> ALCL cells

Analysis of apoptosis by flow cytometry after dual staining with annexin V-FITC and PI showed that at 48 h ASP3026 (0.5, 1.5, and 2.5  $\mu$ M) induced significant apoptosis in Karpas 299, SR-786, and SU-DHL-1 cells (Figure 1C). Apoptosis was also documented by Giemsa staining (Figure 1D).

### ASP3026 decreases the proliferation of NPM-ALK<sup>+</sup> ALCL cells

Karpas 299, SR-786, and SU-DHL-1 cells were treated with ASP3026 and changes in cell proliferation were measured using a BrdU assay. At 48 h, concentration-dependent decreases in cell proliferation were noted in the 3 cell lines (Figure 1E).

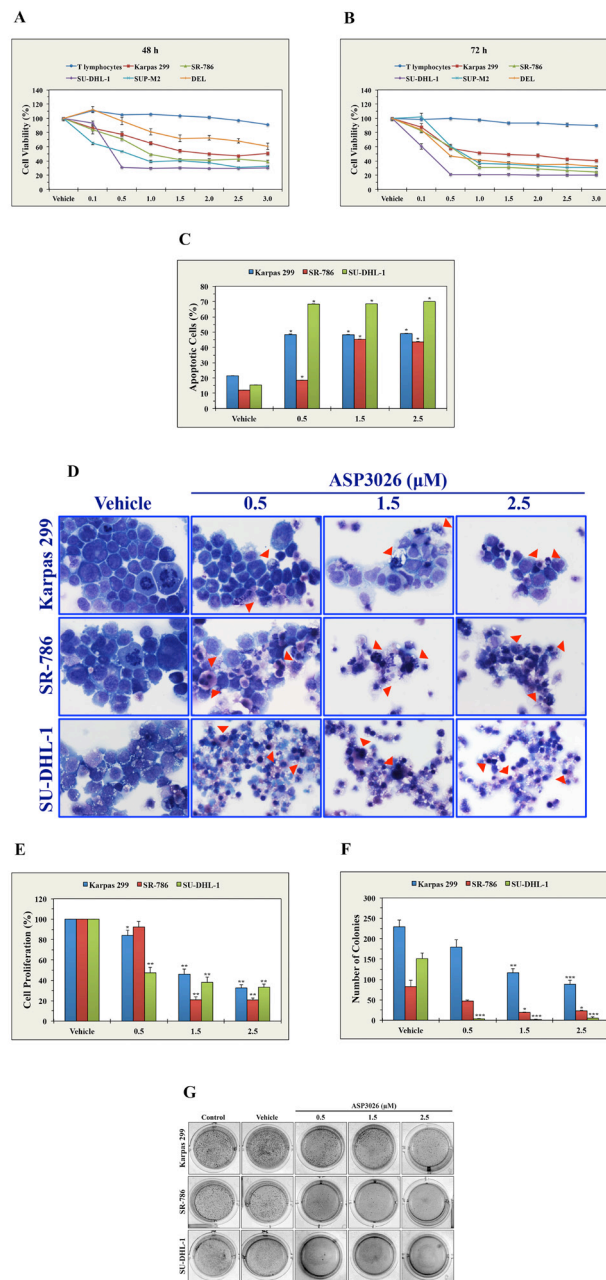


**Figure 1: ASP3026 induces a pronounced negative biological impact in NPM-ALK<sup>+</sup> ALCL cells.** (A) At 48 h, ASP3026 induced concentration-dependent decreases in the viability of NPM-ALK<sup>+</sup> ALCL cells, as measured by MTS assay. These effects were not detected in T lymphocytes, and the decrease in the viability of NPM-ALK<sup>+</sup> ALCL cells was statistically significant compared to T lymphocytes (at 0.1  $\mu\text{M}$  concentration:  $P < 0.05$  in SU-DHL-1,  $P < 0.01$  in Karpas 299,  $P = 0.0001$  in SR-786,  $P < 0.0001$  in SUP-M2,  $P > 0.05$  in DEL [not significant]; at 0.5  $\mu\text{M}$  concentration:  $P < 0.0001$  in all cell lines except DEL where  $P > 0.05$  [not significant]; at  $\geq 1.0 \mu\text{M}$  concentration:  $P < 0.0001$  in all cell lines). (B) The effects of ASP3026 on cell viability were more pronounced at 72 h after treatment (at  $\geq 0.5 \mu\text{M}$ :  $P < 0.0001$  in all cell lines compared with T lymphocytes). (C) Treatment of the NPM-ALK<sup>+</sup> ALCL cells Karpas 299, SR-786, and SU-DHL-1 with ASP3026 for 48 h was associated with significant concentration-dependent increases in apoptotic cell death, as measured by flow cytometry after cellular staining with annexin V/PI (\*:  $P < 0.0001$  compared with vehicle-treated control cells). (D) Morphologic features associated with apoptotic cell death, including cellular shrinkage and nuclear condensation and fragmentation, are shown in Karpas 299, SR-786 and SU-DHL-1 cells after treatment with ASP3026 for 48 h (red arrowheads). (E) ASP3026 also decreased the proliferation of NPM-ALK<sup>+</sup> ALCL cells as measured by BrdU assay (\*:  $P < 0.05$ , \*\*:  $P < 0.0001$  compared with control cells treated with vehicle). (F) Moreover, ASP3026 abrogates anchorage-independent colony formation of NPM-ALK<sup>+</sup> ALCL cells in methylcellulose (\*:  $P < 0.05$ , \*\*:  $P < 0.01$ , \*\*\*:  $P < 0.001$  compared with vehicle-treated control cells). (G) Representative cultures illustrating the marked decrease in the number of NPM-ALK<sup>+</sup> ALCL cell colonies at 5 days after treatment with ASP3026 for 48 h. Results are shown as means  $\pm$  SE of at least 3 consistent experiments.

## ASP3026 abrogates anchorage-independent colony formation of NPM-ALK<sup>+</sup> ALCL cells

Figure 1F shows that treatment with ASP3026 for 48 h induced concentration-dependent decreases in colony numbers in Karpas 299, SR-786, and SU-DHL-1 cells grown for 5 days in methylcellulose. This experiment showed that SU-DHL-1 cells were most sensitive to the effects of ASP3026. Representative images of colonies from untreated cells, cells treated with vehicle, and cells treated with ASP3026 are shown in Figure 1G. Compared with cells treated with vehicle or untreated cells, NPM-ALK<sup>+</sup> ALCL cells treated with ASP3026 developed remarkably fewer colonies.

## ASP3026 reduces the tyrosine kinase activity of NPM-ALK and its phosphorylation levels and induces significant alterations in downstream targets of NPM-ALK signaling

To seek an explanation for the negative biological impact of ASP3026 in NPM-ALK<sup>+</sup> ALCL cells, we measured NPM-ALK tyrosine kinase activity and phosphorylation levels after treatment with ASP3026. ASP3026 induced marked decreases in the tyrosine kinase activity of NPM-ALK in Karpas 299, SR-786, and SU-DHL-1 cells (Figure 2A). Furthermore, Western

blotting results showed that ASP3026 downregulated pNPM-ALK at Y646 and Y664 (Figure 2B). Moreover, ASP3026 induced remarkable downregulation of the phosphorylation of several survival-promoting proteins that are known to be activated by NPM-ALK including IGF-IR, STAT3, AKT, and JNK (Figure 2B). The occurrence of apoptosis after treatment with ASP3026 was biochemically supported by cleavage of caspase 3 and PARP (Figure 2B).

## ASP3026 decreases the proliferation of 293T cells transfected with crizotinib-resistant NPM-ALK mutants

To test whether ASP3026 can overcome the resistance to crizotinib, we used crizotinib or ASP3026 to treat 293T cells transiently transfected with NPM-ALK, NPM-ALK<sup>I231N</sup> or NPM-ALK<sup>L256Q</sup>. Not surprisingly, crizotinib (Figure 3A) and ASP3026 (Figure 3B) induced concentration-dependent decrease in the proliferation of cells transfected with NPM-ALK. Whereas ASP3026 efficiently decreased the proliferation of cells transfected with NPM-ALK<sup>I231N</sup> or NPM-ALK<sup>L256Q</sup>, crizotinib failed to induce similar effects. To further analyze the differential effects of crizotinib and ASP3026, we studied the changes in pNPM-ALK levels. Indeed, crizotinib and ASP3026 caused marked downregulation of pNPM-ALK at Y664 in 293T cells transfected with NPM-ALK. Nonetheless, only

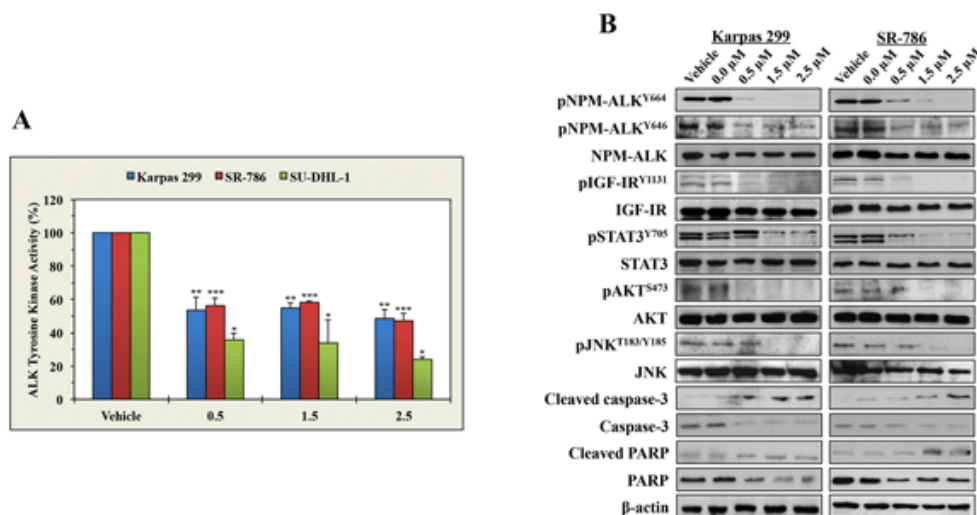


**Figure 2: ASP3026 reduces the tyrosine kinase activity of NPM-ALK, downregulates the phosphorylation of NPM-ALK and target proteins, and induces biochemical effects consistent with apoptosis.** (A) ASP3026 induced a marked decrease in NPM-ALK tyrosine kinase activity in the lymphoma cells (\*:  $P < 0.01$ , \*\*:  $P < 0.001$ , \*\*\*:  $P < 0.0001$  compared with control cells treated with vehicle). Results shown are means  $\pm$  SE of 3 experiments. (B) ASP3026 decreased the phosphorylation of NPM-ALK at 2 different tyrosine residues: Y646 and Y664. Also, treatment with ASP3026 was associated with downregulation of the phosphorylation of the NPM-ALK target proteins IGF-IR, STAT3, AKT, and JNK. Changes in the basal levels of these proteins were not detected. The occurrence of apoptosis was biochemically supported by the increase in cleaved caspase-3 and cleaved PARP and the simultaneous decrease in non-cleaved caspase-3 and non-cleaved PARP levels.  $\beta$ -Actin indicates equal loading of the proteins.

ASP3026 was capable of reducing pNPM-ALK levels at Y664 in cells transfected with NPM-ALK<sup>I231N</sup> or NPM-ALK<sup>L256Q</sup> (Figure 3C). Densitometry of the Western blot bands is shown (Figures 3D and 3E).

### ASP3026 suppresses NPM-ALK<sup>+</sup> ALCL tumor growth *in vivo*

Female C.B-17 SCID mice were randomized into 4 treatment groups (control [10 mice]; uninterrupted ASP3026 [U, 5]; interrupted ASP3026 [I, 5]; and CHOP [10]) at 3 weeks after intravenous injection of Karpas 299 cells permanently expressing firefly luciferase (Figure 4A).

Lymphoma tumor burden was monitored weekly

using bioluminescence imaging and detection of signal intensity. ASP3026-treated mice demonstrated remarkable lymphoma regression at 2 weeks after treatment initiation. Mice treated uninterruptedly with ASP3026 demonstrated complete remission with no relapse or lymphoma-related death. Representative examples are shown in Figure 4B (lanes 1 & 2). Notably, ALCL relapsed as early as 1 week after interruption of ASP3026 (examples shown in Figure 4B; lanes 3-6). Two mice with relapse were euthanized at week 8 owing to heavy tumor burden (Figure 4B; lanes 3 & 4). At week 9, ASP3026 was re-administered to the other 3 mice; their tumors substantially regressed and they lived until study termination (examples shown in Figure 4B; lanes 5 & 6). The inhibitory effects of ASP3026 on NPM-ALK<sup>+</sup> ALCL growth were attributable, at least in

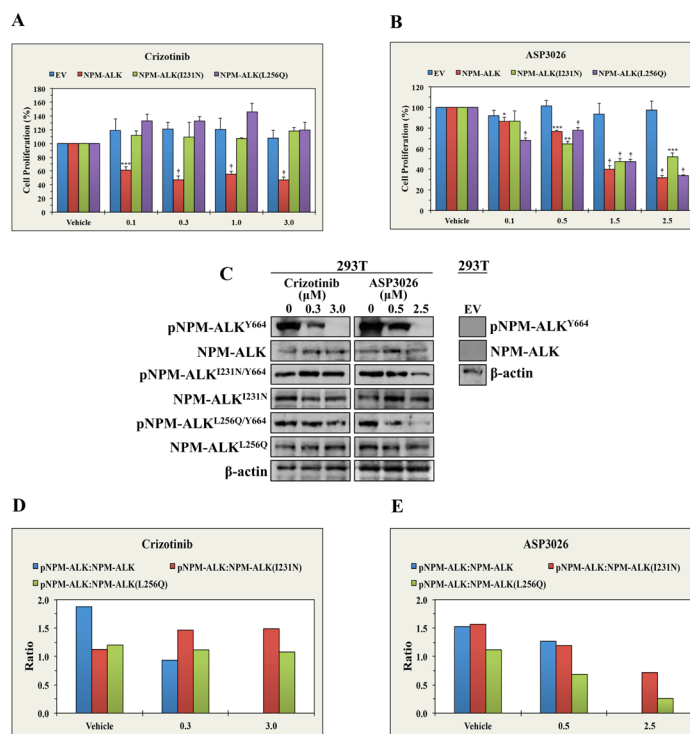


**Figure 3: ASP3026 overcomes the resistance to crizotinib in NPM-ALK<sup>+</sup> ALCL.** (A) Whereas crizotinib induced significant decrease in the proliferation of 293T cells transiently transfected with NPM-ALK, it failed to induce similar effects in the cells transfected with EV, NPM-ALK<sup>I231N</sup> or NPM-ALK<sup>L256Q</sup>. (B) ASP3026 successfully decreased the proliferation of 293T cells transfected with NPM-ALK, NPM-ALK<sup>I231N</sup> or NPM-ALK<sup>L256Q</sup> (\*:  $P < 0.05$ , \*\*:  $P < 0.01$ , \*\*\*:  $P < 0.001$ , †:  $P < 0.0001$ ). No effects were seen when control 293T cells transfected with EV were treated with ASP3026. Results represent the means  $\pm$  SE of 3 experiments. (C) The left panel shows that crizotinib decreased the phosphorylation of NPM-ALK transfected in 293T cells, but not the phosphorylation of NPM-ALK<sup>I231N</sup> or NPM-ALK<sup>L256Q</sup>. At the other hand, ASP3026 reduced the phosphorylation of the three constructs. The levels of non-phosphorylated NPM-ALK constructs and  $\beta$ -actin support equal protein loading. The right panel illustrates lack of NPM-ALK/pNPM-ALK protein expression in 293T cells transfected with EV. (D) Densitometric analysis depicting the ratio of pNPM-ALK Western blot bands to their corresponding NPM-ALK bands is shown. The results illustrate that crizotinib induced remarkable downregulation of pNPM-ALK in 293T cells transfected with NPM-ALK but not in 293T cells transfected with crizotinib-resistant NPM-ALK mutants. (E) Furthermore, the densitometric analysis also shows that treatment with ASP3026 caused concentration-dependent decrease in pNPM-ALK levels in cells transfected with NPM-ALK, NPM-ALK<sup>I231N</sup> or NPM-ALK<sup>L256Q</sup>.

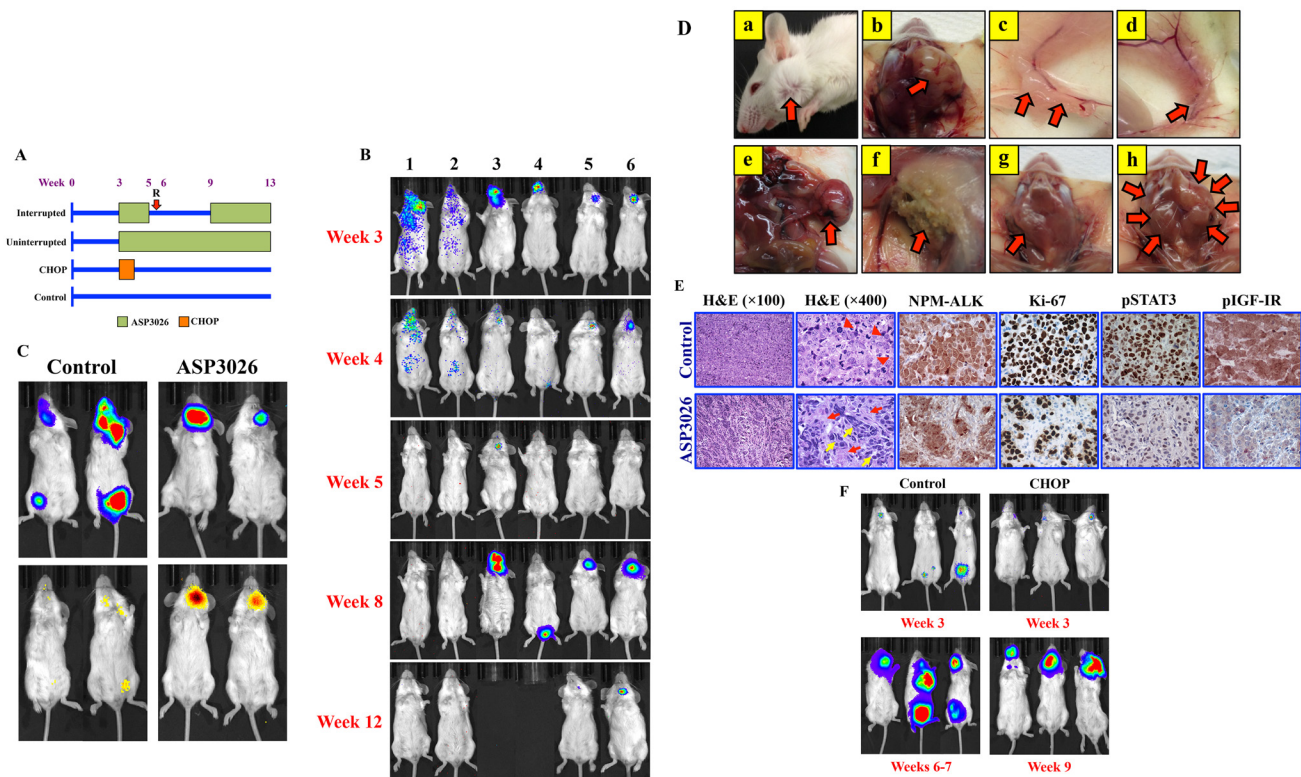


**Figure 4: ASP3026 suppresses NPM-ALK<sup>+</sup> ALCL tumor cell growth *in vivo*.** (A) C.B-17 SCID mice were randomized into the 4 illustrated treatment groups at week 3 after intravenous injection of Karpas 299 cells permanently expressing firefly luciferase. “R” denotes relapse after ASP3026 discontinuation. (B) Mice developed NPM-ALK<sup>+</sup> ALCL tumors within approximately 3 weeks after injection, and were monitored weekly using bioluminescence imaging. The intensity of the signal is indicated by color (blue: low; green: intermediate; red: high tumor burden). Mice uninterruptedly treated with ASP3026 (examples shown in lanes 1 & 2) underwent complete remission with no relapse until study termination at week 13. Administration of ASP3026 was interrupted in 5 mice (examples in lanes 3-6) for 4 weeks. Notably, ALCL relapsed as early as 1 week after discontinuation of ASP3026. Two mice (lanes 3 & 4) had to be euthanized before the study period ended because of relapsed NPM-ALK<sup>+</sup> ALCL with extensive tumor burden. At week 9, ASP3026 was re-administered in the other 3 mice (2 shown in lanes 5 & 6), and the NPM-ALK<sup>+</sup> ALCL tumors substantially regressed, and the mice survived until termination of the study. (C) Bioluminescence imaging highlights the NPM-ALK<sup>+</sup> ALCL tumors in control and ASP3026-treated mice (upper panels). Mice were injected intraperitoneally by the firefly luciferase prosubstrate VivoGlo Caspase-3/7 and bioluminescence imaging was performed. Tumors in control mice treated only with vehicle failed to demonstrate significant apoptosis signals (left lower panel). In contrast, intense signals consistent with marked *in vivo* lymphoma cell apoptosis were detected in mice treated with ASP3026 (right lower panel). (D) Examples of control mice showing lymphoma (red arrows) in cervical lymph nodes (a, exterior; b, dissected); inguinal lymph nodes (c, d); mesenteric lymph nodes (e); and axillary lymph nodes (f). Example of cervical lymph nodes is shown in a mouse treated interruptedly with ASP3026 (group I). After relapse, this mouse received ASP3026, survived, and was euthanized at the end of the study. A small cervical lymph node (red arrow) was detected at necropsy (g). This lymph node was processed and microscopically examined as shown in Figure 3E, lower panel. Example of cervical lymph nodes is shown after relapse in a mouse treated interruptedly with ASP3026. The lymph nodes comprised large, bulky tumor masses (red arrows) (h). (E) Histologic sections from cervical lymph node obtained from a control mouse treated with vehicle show effacement of the normal nodal architecture by solid sheets of lymphoma cells (H&E staining; original magnification:  $\times 100$ ). Higher magnification shows large cells with abundant cytoplasm, vesicular nuclei, and high mitotic rate with atypical mitotic figures [red arrowheads] (H&E;  $\times 400$ ). Immunohistochemical staining shows cytoplasmic and nuclear localization of NPM-ALK protein in the solid sheets of the lymphoma cells. Ki-67 is expressed in the vast majority of the lymphoma cells that diffusely infiltrate the lymph node. In addition, pSTAT3<sup>Y705</sup> and pIGF-IR<sup>Y1161</sup> are highly expressed in almost all of the lymphoma cells. Also shown are histologic sections from a small post-treatment cervical lymph node collected at necropsy from a mouse treated with ASP3026 after relapse (I group, illustrated in Figure 3D, panel g). H&E staining shows small nests of ALCL cells separated by thick stromal tissue strands ( $\times 100$ ). Higher magnification of the same lymph node further illustrates the small clusters of lymphoma cells with rare mitotic figures [yellow arrows] separated by thick stromal strands that include fibroblasts, small blood vessels, and admixed inflammatory cells [red arrows] ( $\times 400$ ). Although NPM-ALK and Ki-67 were identified in residual ALCL cells, the numbers of these cells were much less pronounced after treatment. The expressions of pSTAT3 and pIGF-IR are substantially reduced in the lymph node sections from the ASP3026-treated mouse. Immunohistochemical staining photomicrographs are shown at an original magnification of  $\times 400$ . (F) Control mice at week 3 (top left) and weeks 6-7 (bottom left) show remarkable progression of systemic NPM-ALK<sup>+</sup> ALCL. Examples of mice from the CHOP-treatment group with NPM-ALK<sup>+</sup> ALCL established at week 3 (top right). Although CHOP initially suppressed NPM-ALK<sup>+</sup> ALCL tumor growth, lymphoma relapsed as illustrated at week 9 and the mice had to be euthanized because of heavy tumor burden (bottom right).

part, to *in vivo* apoptotic cell death (Figure 4C; right lane). Significant apoptosis was not observed in control mice treated with vehicle (Figure 4C; left lane). The occurrence of disseminated systemic lymphoma in cervical, inguinal, mesenteric, and axillary lymph nodes from control mice was confirmed at necropsy (Figure 4D, panels a-f). Figure 4D, panel g, shows a small cervical lymph node from a mouse from the interrupted (I) ASP3026 group that developed relapsed lymphoma and thereafter was treated with ASP3026 and survived until the termination of the study. Figure 4D, panel h, illustrates markedly enlarged cervical lymph nodes involved with lymphoma in a mouse from the interrupted ASP3026 group (I) after relapse. This mouse was euthanized before the end of the study because of heavy tumor burden.

Histologic examination of tissues obtained from control mice showed infiltration by solid sheets of malignant lymphoma cells (Figure 4E). Expression of ALK was confirmed by immunohistochemical analysis (Figure 4E). Ki-67 was expressed in the vast majority of the lymphoma cells that diffusely infiltrated the tissues. In addition, strong expressions of pSTAT3 and pIGF-IR were detected in most of the lymphoma cells (Figure 4E). Conversely, tissues from a mouse from the interrupted ASP3026 group (I) that was treated with ASP3026 after relapse (lymph node is shown in figure 4D, panel g) illustrated that treatment with ASP3026 was associated with marked decrease in the number of tumor cells. Instead of the solid ALCL sheets seen in control lymph nodes; after treatment with ASP3026, scattered nests of ALCL cells separated by thick stromal strands were detected (Figure 4E). Although ALK and Ki-67 were present in

residual ALCL cells in the treated tumors, their numbers were much lower. Moreover, the expression of pSTAT3 and pIGF-IR were markedly decreased after treatment with ASP3026 (Figure 4E).

In another group, NPM-ALK<sup>+</sup> ALCL tumor-bearing mice were treated with CHOP. Although CHOP initially suppressed NPM-ALK<sup>+</sup> ALCL tumor growth, aggressive lymphoma later relapsed and the mice had to be euthanized before completion of the study because of heavy tumor burden. Figure 4F shows examples of control mice and mice treated with CHOP.

### Treatment with ASP3026 causes superior survival in mice engrafted with systemic NPM-ALK<sup>+</sup> ALCL

Whereas control mice survived  $43.1 \pm 3.3$  (mean  $\pm$  SE) days from study inception and mice treated with CHOP survived  $50.6 \pm 6.4$  days, mice treated with ASP3026 (U) survived  $79.8 \pm 8.0$  days, and those treated with ASP3026 (I) survived  $77.8 \pm 8.1$  days (Fig. 5A). Kaplan-Meier survival curves (Figure 5B) show that mice treated with ASP3026 (U or I) had superior overall survival compared with mice treated with vehicle or CHOP.

## DISCUSSION

In the present study, we adopted comprehensive *in vitro* and *in vivo* experimental approaches that allowed in depth characterization of the effects of the recently

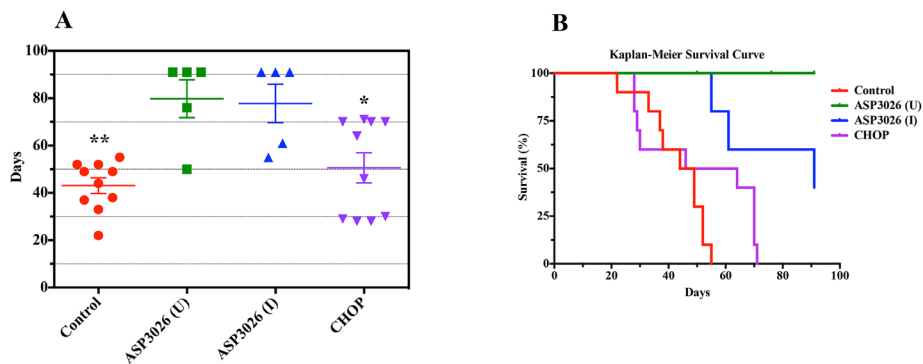


**Figure 5: Treatment with ASP3026 is associated with superior overall survival in NPM-ALK<sup>+</sup> ALCL.** (A) Scatterplot shows that the mean  $\pm$  SE duration of survival in control mice was  $43.1 \pm 3.3$  days. Mice treated with CHOP lived slightly longer ( $50.6 \pm 6.4$  days). In contrast, mice treated with uninterrupted ASP3026 (U) lived  $79.8 \pm 8.0$  days and those treated with interrupted ASP3026 (I) lived  $77.8 \pm 8.1$  days. Two mice treated with ASP3026 (U) died incidentally at 50 and 76 days because of infection, with no evidence of lymphoma tumors by imaging or by complete necropsy. In the ASP3026 (I) group, mice developed relapsed lymphoma after the interruption of ASP3026, and 2 mice were euthanized at 55 and 61 days because of extensive tumor burdens. The other 3 mice received ASP3026 after relapse and the lymphoma regressed. These mice survived until the termination of the study (\*:  $P < 0.05$ ; \*\*:  $P < 0.01$  vs. ASP3026 [U or I]). (B) Kaplan-Meier survival curves show that mice treated with ASP3026 (U or I) demonstrated statistically superior overall survival compared with control mice treated with vehicle or CHOP ( $P = 0.001$  in ASP3026 [U] vs. control or CHOP;  $P = 0.001$  in ASP3026 [I] vs. control;  $P = 0.04$  in ASP3026 [I] vs. CHOP). Significance differences were not detected between control mice and mice treated with CHOP or between mice treated with ASP3026 (U) and mice treated with ASP3026 (I).

developed ALK inhibitor ASP3026 in NPM-ALK<sup>+</sup> ALCL. Our *in vitro* experiments demonstrated that ASP3026 causes a marked decrease in the viability of NPM-ALK<sup>+</sup> ALCL cells, which could be at least partially explained by a significant increase in apoptotic cell death. Also, ASP3026 induces a significant decrease in cellular proliferation and anchorage-independent colony formation in NPM-ALK<sup>+</sup> ALCL. Although all of the NPM-ALK<sup>+</sup> ALCL cell lines used in this study demonstrated significant *in vitro* responses to ASP3026, some assays showed variable sensitivities of the different cell lines to the effects of ASP3026. Previous reports highlighted inherent biochemical differences between NPM-ALK<sup>+</sup> ALCL cell lines that could explain their variable sensitivities to inhibitors of lymphoma cell survival [26].

When the direct effects of ASP3026 on NPM-ALK were examined, we found remarkable decreases in NPM-ALK tyrosine kinase activity and tyrosine phosphorylation levels at 2 residues, Y646 and Y664. It has been previously shown that Y664 is functionally relevant as it is the residue where NPM-ALK binds with survival-promoting proteins such as phospholipase C- $\gamma$  and IGF-IR [27-29]. Downregulation of the phosphorylated form of NPM-ALK by ASP3026 was associated with a remarkable reduction in the phosphorylation levels of IGF-IR, STAT3, AKT, and JNK proteins, which are established targets of NPM-ALK signaling that contribute significantly to the survival of this lymphoma [28-33]. At the biochemical level, ASP3026 successfully induced cleavage of caspase 3 and PARP, further indicating that it induces apoptosis in NPM-ALK<sup>+</sup> ALCL cells.

To analyze the effects of ASP3026 *in vivo*, we generated and utilized a systemic NPM-ALK<sup>+</sup> ALCL model in SCID mice and monitored tumor development using a bioluminescence-based imaging system. Contrary to the widely utilized NPM-ALK<sup>+</sup> ALCL xenograft models that exploit localized, subcutaneous tumor engrafts [34, 35], our approach is much more relevant to clinical settings where NPM-ALK<sup>+</sup> ALCL patients typically present with widely disseminated disease. Uninterrupted oral administration of ASP3026 was associated with total eradication of established systemic lymphoma tumors with no evidence of relapse throughout the entire period of the study. In mice where ASP3026 was withheld after 2 weeks of daily administration, NPM-ALK<sup>+</sup> ALCL tumors quickly relapsed, indicating that tumor suppression was secondary to the administration of ASP3026. Nonetheless, when treatment was resumed in some of these mice, lymphoma growth decreased significantly and the mice survived until study termination. In contrast to ASP3026-treated mice, mice treated with vehicle developed aggressive systemic lymphoma and had to be euthanized before study period ended. Importantly, we also evaluated the response of NPM-ALK<sup>+</sup> ALCL to the commonly utilized CHOP regimen. Although the lymphoma initially regressed in response to CHOP, it eventually relapsed and mice had to

be euthanized before study termination.

Histologic evaluation of NPM-ALK<sup>+</sup> ALCL tumors in mice undergoing treatment with ASP3026 showed response to therapy in the form of much less proliferative lymphoma cells than those observed in control mice. Furthermore, immunohistochemical staining demonstrated that pSTAT3 and pIGF-IR expressions were significantly weakened in tumors collected after ASP3026 treatment, which supports the Western blotting data from the *in vitro* experiments.

NPM-ALK<sup>+</sup> ALCL is an aggressive neoplasm. Although patients show a favorable response to CHOP, 30-40% of patients subsequently develop resistance, have multiple relapses, and frequently die. Factors that have been associated with poor outcome include stage III/IV disease at presentation, involvement of the mediastinum, viscera or skin, and elevated LDH levels [7, 12]. More recent studies have shown that the presence of specific molecular events at presentation or during therapy could distinguish subgroups of NPM-ALK<sup>+</sup> ALCL patients with worse prognosis. For instance, detection of *NPM-ALK* transcripts in bone marrow or serum (i.e., minimal disseminated disease [MDD]) and levels of anti-NPM-ALK antibody in serum at diagnosis were used to stratify 128 patients into high-, intermediate- or low-risk groups. High- and intermediate-risk patients represented 20% and 31%, respectively, of this patient cohort. The progression-free survival rates were 28% and 68% in these 2 groups, respectively [36]. Furthermore, patients with MDD at diagnosis and minimal residual disease after their first course of CHOP-based chemotherapy showed an 81% cumulative incidence of relapse and only had a 65% 5-year overall survival rate [37]. These findings stress the urgent need to develop more specific and effective approaches to treat NPM-ALK<sup>+</sup> ALCL.

Considering that the number of currently available ALK inhibitors is limited [38, 39], it is very important to study these inhibitors in different types of ALK<sup>+</sup> tumors to determine their utility in clinical settings. Crizotinib is one of the most extensively studied ALK inhibitors; nonetheless, it has been more evaluated in ALK<sup>+</sup> solid tumors [16-18]. Although crizotinib demonstrated excellent efficacy in eradicating EML4-ALK<sup>+</sup> NSCLC tumors, recent reports have stressed the evolution of EML4-ALK mutations that are substantially resistant to crizotinib [21-23]. Indeed, several mechanisms, including somatic kinase domain mutations, *ALK* gene fusion copy number gain, and the emergence of separate oncogenic drivers, have been implicated in the initiation of crizotinib resistance [21-23, 40-43]. Resistance to crizotinib has also been reported in patients with inflammatory myofibroblastic tumor who presented with the BARBP2-ALK translocation and developed the ALK<sup>F1174L</sup> activation mutation after treatment with crizotinib [44]. Notably, this mutation also resides in a subgroup of neuroblastoma patients, where it confers resistance to crizotinib [45].

More recently, resistance to crizotinib has also been described in NPM-ALK<sup>+</sup> ALCL [46, 47]. Culturing NPM-ALK<sup>+</sup> ALCL cell lines in increasing concentrations of crizotinib resulted in the evolution of 2 acquired mutants – NPM-ALK<sup>I231N</sup> and NPM-ALK<sup>L256Q</sup> – that were remarkably resistant to crizotinib [46]. Furthermore, the NPM-ALK<sup>I231N</sup> mutant was also identified in a lymphoma patient who was receiving crizotinib [47]. Our data show that ASP3026 effectively decreased the proliferation of 293T cells expressing these mutants. In addition, ASP3026 was capable of decreasing the phosphorylation of crizotinib-resistant NPM-ALK mutants at Y664. Considering that therapeutic resistance is a major hurdle for clinical utilization of crizotinib, these promising findings suggest that ASP3026 could be used to overcome crizotinib resistance in NPM-ALK<sup>+</sup> ALCL.

In summary, we performed extensive *in vitro* and *in vivo* analyses of the effects of ASP3026 on the survival and growth of NPM-ALK<sup>+</sup> ALCL. Our results provide strong evidence that ASP3026 could represent a novel and successful therapeutic strategy to eradicate this aggressive lymphoma and that patients with NPM-ALK<sup>+</sup> ALCL, including those with crizotinib resistance, should be enrolled in the current clinical trials testing the effects of ASP3026 in ALK<sup>+</sup> neoplasms.

## METHODS

### Cell lines

The NPM-ALK<sup>+</sup> T-cell ALCL cell lines Karpas 299, SU-DHL-1, SUP-M2, SR-786, and DEL were purchased from DSMZ (Braunschweig, Germany). The 293T cells (ATCC, Manassas, VA) were used in transfection experiments. Human peripheral blood CD3<sup>+</sup> pan-T lymphocytes were used in some experiments (catalogue number: PB009-1F) (StemCell Technologies, Vancouver, BC, Canada). The lymphoma cell lines and T lymphocytes were maintained in RPMI 1640 supplemented with 10% FBS, 2 mM glutamine, 100 U/mL penicillin, and 100 µg/mL streptomycin, and then incubated at 37°C in 5% CO<sub>2</sub>. 293T cells were maintained in DMEM under similar conditions.

### ALK inhibitor

ASP3026 (CT-ASP302; ChemieTek, Indianapolis, IN) was suspended in DMSO admixed with H<sub>2</sub>O and HCl (1:1) for *in vitro* experiments and in 0.5% methylcellulose for *in vivo* experiments.

### Antibodies

The following antibodies were purchased: pALK<sup>Y1604</sup> (Y664 in NPM-ALK; 3341), pALK<sup>Y1586</sup> (Y646 in NPM-ALK; 3343), pIGF-IR<sup>Y1131</sup> (3021), pSTAT3<sup>Y705</sup> (4113), AKT (9272), pAKT<sup>S473</sup> (4051), JNK (3708S), pJNK<sup>T183/Y185</sup> (4668S), PARP (9542P), cleaved PARP (5625S), and cleaved caspase-3 (9661S) (Cell Signaling Technology, Danvers, MA); pIGF-IR<sup>Y1161</sup> (Ab39398) (Abcam, Cambridge, MA); IGF-IR (39-6700) (Invitrogen, Grand Island, NY); STAT3 (sc-8019) and caspase-3 (sc-7272) (Santa Cruz Biotechnology, Santa Cruz, CA); ALK (M719501-2) and Ki-67 (M7240) (Dako, Carpinteria, CA); and β-actin (A-2228) (Sigma-Aldrich, St. Louis, MO).

### MTS assay

Cell viability was measured using MTS reagent (3-(4,5-dimethylthiazol-2-yl)-5-(3-carboxymethoxyphenyl)-2-(4-sulfophenyl)-2H-tetrazolium; Promega, Madison, WI). Briefly, 1 × 10<sup>5</sup> cells were seeded into 96-well plates, and 20 µL of MTS reagent was added to each well and incubated for approximately 2 h at 37°C in 5% CO<sub>2</sub>. Plates were read at 490 nm.

### *In vitro* apoptosis detection

Cytospin preparations were stained by Wright-Giemsa and analyzed by light microscopy for morphologic features consistent with apoptosis. Apoptosis was also detected using a commercially available kit (556547, BD Biosciences, San Jose, CA). Cells were stained with annexin V-FITC and propidium iodide (PI) and incubated at room temperature for 15 min in annexin binding buffer. Analysis was performed using flow cytometry (BD FACSCalibur) and CellQuest software (BD Biosciences).

### BrdU assay

Cell proliferation was measured using a standard kit (X1327K1, Exalpha Biologicals, Shirley, MD). Cells were plated at a concentration of 2 × 10<sup>5</sup> cells/well after which 20 µL of BrdU (1:500 in cell culture medium) was added for 24 h. Plates were centrifuged for 5 min, fixed, and washed. Then, 100 µL of anti-BrdU antibody was added for 1 h, followed by 100 µL of peroxidase goat anti-mouse IgG conjugate (1:2000) for 30 min and then 100 µL of 3,3',5,5'-tetramethylbenzidine (TMB) substrate for 30 min. Stop solution (50 µL) was added, and the plates were read at 450/595 nm using an ELISA plate reader.

**Table 1: Primer sequences for crizotinib-resistant NPM-ALK mutants.**

NPM-ALK<sup>I231N</sup>: F, 5'-GGAAGCCCTGATCAATAGCAAATTCAACCACCAAGAAC-3';  
R, 5'-GTTCTGGTGGTTGAATTTGCTATTGATCAGGGCTTCC-3'  
NPM-ALK<sup>L256Q</sup>: F, 5'-CAATCCCTGCCCCGGTTCATCCTGCAGGAGCTCATGGCGGG-3';  
R, 5'-CCCCCATGAGCTCCTGCAGGATGAACCGGGGCAGGGATTG-3'.

### Anchorage-independent colony formation

Cells were treated with vehicle or ASP3026 for 48 h and then plated in methylcellulose-based medium (Methocult H4230; Stemcell Technologies) mixed in RPMI 1640 (1:5). Harvested cells were suspended in methylcellulose (v/v; 1:10) and poured into 24-well plates. The plates were incubated for 5 days at 37°C in 5% CO<sub>2</sub>. Colonies were stained using p-iodonitrotetrazolium violet and visualized using the FluorChem 8800 imaging system (Alpha Innotech, San Leandro, CA).

### Tyrosine kinase assay

NPM-ALK tyrosine kinase activity was measured using the Universal Tyrosine Kinase Assay Kit (Takara Bio, Pittsburg, PA). Briefly, 2 × 10<sup>6</sup> cells were immunoprecipitated using standard protocol and ALK antibody (Dako) overnight at 4°C. Samples were spun and resuspended (including beads) in Kinase Reacting Solution and plated in triplicates in the protein tyrosine kinase substrate immobilized microplate (provided in the kit). ATP-2Na was added to each well in order to start tyrosine phosphorylation and incubated at 37°C for 30 min. The sample solution was then aspirated, and the wells were washed 4 times. Subsequently, samples were blocked with blocking solution for 30 min at 37°C, followed by addition of 50 µL of anti-phosphotyrosine (PY20)-horseradish peroxidase (HRP) solution for 30 min at 37°C. Finally, samples were washed and 100 µL of the HRP substrate TMB was added into each well for 15 min. The reaction was stopped by adding 100 µL of stop solution and absorbance was measured at 450 nm.

### Western blotting

The lysis buffer contained 25 mM HEPES (pH 7.7), 400 mM NaCl, 1.5 mM MgCl<sub>2</sub>, 2 mM EDTA, 0.5% Triton X-100, 0.1 mM phenylmethylsulfonyl fluoride, 3 mM dithiothreitol, phosphatase and protease inhibitor cocktails. Fifty to 80 µg total proteins were electrophoresed on 8% SDS-PAGE, transferred onto polyvinylidene fluoride membranes, and probed with primary antibodies and then matched secondary antibodies conjugated with HRP. Protein expression was detected using chemiluminescence and a commercially available kit (GE Healthcare, Piscataway, NJ).

### Site-directed mutagenesis

To generate the crizotinib-resistant NPM-ALK<sup>I231N</sup> and NPM-ALK<sup>L256Q</sup> mutants that are equivalent to ALK<sup>I1171N</sup> and ALK<sup>L1196Q</sup>, a wild type NPM-ALK plasmid and the Quick Change II XL Site Directed Mutagenesis kit were used (Agilent Technologies, Santa Clara, CA) [28, 46, 47]. Primer sequences are depicted in Table 1. Five-µL of the PCR products were transformed using MaxEfficiency DH5α competent cells (Invitrogen), and the transformation reactions were plated in ampicillin resistant plates overnight at 37°C. Colonies containing the correct inserts, as determined by sequencing, were amplified overnight at 37°C in LB Broth containing ampicillin, and subjected to purification by using the Qiaprep Spin Miniprep Kit (Qiagen). Optical densities were acquired using spectrophotometry (NanoDrop 2000, Thermo Scientific, Waltham, MA).

### Transfection

Briefly, 293T cells (1 × 10<sup>6</sup>) were plated in 6 well plates 24 h prior to transfection. Then, 2 µg of wild type NPM-ALK, NPM-ALK<sup>I231N</sup> or NPM-ALK<sup>L256Q</sup> were added to 100 µL OptiMEM medium. Simultaneously, 7 µL of Lipofectamine (Invitrogen) were added to 100 µL OptiMEM medium in a different tube. After incubation for 5 min at room temperature, the contents of the 2 tubes were admixed and incubated for 20 min at room temperature. The mixture was added to the corresponding well.

### Systemic xenograft NPM-ALK<sup>+</sup> ALCL model

*In vivo* studies were preapproved by our Institutional Animal Care and Use Committee. Karpas 299 cells permanently expressing firefly luciferase and green fluorescence protein (GFP) were generated by using the F-Luc-GFP lentivirus (Capital Biosciences, Rockville, MD) in which humanized firefly luciferase (hLuc) was expressed under the CMV promoter. GFP and puromycin resistance marker were co-expressed bicistronically under the SV40 promoter [48]. Cells (1 × 10<sup>6</sup>/mouse) were injected into the tail veins of female C.B-17 SCID mice (6-8 weeks old; Taconic, Cambridge City, IN). Most of the mice developed NPM-ALK<sup>+</sup> ALCL at approximately 3 weeks after injection. Lymphoma was monitored by luciferase signaling detection upon intraperitoneal

injection of D-luciferin (Gold Biotechnology, St. Louis, MO) using bioluminescence imaging (IVIS Lumina XR imaging system; Caliper Life Sciences, Alameda, CA). ASP3026 (30 mg/kg daily) was administered using oral gavage at 3 weeks after injection of Karpas 299 cells. In one group (U), ASP3026 was administered uninterruptedly for 10 weeks, and in a second group (I), it was given for 2 weeks, interrupted for 4 weeks, and then continued for an additional 4 weeks. Control mice were given vehicle (0.5% methylcellulose). In a fourth group, CHOP [cyclophosphamide (40 mg/kg), doxorubicin (3.3 mg/kg), and vincristine (0.5 mg/kg) were given intravenously; and prednisone (0.2 mg/kg) was given by oral gavage] was administered for 5 consecutive days 3 weeks after injection of the lymphoma cell line [49, 50]. Tumor progression was monitored every week until death or until the study was concluded at week 13. The mice were euthanized and a total body necropsy was performed. Tumors were excised and fixed in 10% buffered formalin or snap-frozen in liquid nitrogen.

### ***In vivo* apoptosis detection**

Apoptosis detection in mice was performed by intraperitoneal injection of the firefly luciferase prosubstrate VivoGlo Caspase-3/7 (P1781; Z-DEVD-Aminoluciferin, Promega) and bioluminescence imaging (IVIS Lumina XR imaging system; Caliper Life Sciences).

### **Immunohistochemical staining**

Formalin-fixed and paraffin-embedded tissue sections from mouse lymphoma tumors were deparaffinized using an alcohol gradient. Sections were subsequently washed and subjected to antigen retrieval for 20 min in a steamer using 1× Target Retrieval Solution (Dako) and then allowed to cool down for 20 min to room temperature, washed, and incubated in 3% H<sub>2</sub>O<sub>2</sub> for 15 min to block endogenous peroxidase activity. The sections were then blocked in serum-free blocking solution (Universal LSAB+ kit, Dako) for 30 min at room temperature. Primary antibody diluted in blocking buffer (1:50 for ALK and pSTAT3; 1:100 for pIGF-IR and Ki-67) was added for overnight incubation at 4°C. Next, the sections were washed 3 times and incubated with the secondary antibody LINK and then with secondary antibody streptavidin each for 30 min, and developed with 3,3'-diaminobenzidine tetrahydrochloride substrate that includes HRP. Hematoxylin was used for counterstaining.

### **Statistical analysis**

Survival analysis was performed using PRISM software (GraphPad, La Jolla, CA) and the generation

of Kaplan-Meier curves. The significance of differences between the groups was assessed using the Mantel-Cox log-rank test. For other data, statistical significance was detected by using one-way analysis of variance and the Bonferroni's post hoc multiple comparisons test.  $P < 0.05$  was considered statistically significant.

### **Authorship**

S.K.G., D.V. participated in developing the conception of the study, designed experiments, performed research, analyzed data, and contributed to writing the paper; R.M. performed research; P.S. participated in developing the conception of the study, designed experiments, and analyzed data; H.M.A. developed the conception of and supervised the study, provided essential experimental tools, designed experiments, performed research, analyzed data, and wrote the paper. The authors declare no competing financial interests.

### **ACKNOWLEDGMENTS**

We are grateful to Dawn Chalaire for outstanding assistance with the preparation of this paper. The authors also thank Jessica G. Granda, B.S., and Bin Shi, Ph.D., for providing technical support. This work was supported by an R01 CA151533 grant from the National Cancer Institute to H.M.A. The contents of this paper are solely the responsibility of the authors and do not necessarily represent the official views of the National Cancer Institute or the National Institutes of Health.

### **Editorial Note**

This paper has been accepted based in part on peer-review conducted by another journal and the authors' response and revisions as well as expedited peer-review in *Oncotarget*.

### **REFERENCES**

1. Iwahara T, Fujimoto J, Wen D, Cupples R, Bucay N, Arakawa T, Mori S, Ratzkin B, Yamamoto T. Molecular characterization of ALK, a receptor tyrosine kinase expressed specifically in the nervous system. *Oncogene*. 1997; 14: 439-449.
2. Souttou B, Carvalho NB, Raulais D, Vigny M. Activation of anaplastic lymphoma kinase induces neuronal differentiation through the mitogen-activated protein kinase pathway. *J Biol Chem*. 2001; 276: 9526-9531.
3. Amin HM, Lai R. Pathobiology of ALK+ anaplastic large-cell lymphoma. *Blood*. 2007; 110: 2259-2267.
4. Morris SW, Kirstein MN, Valentine MB, Dittmer KG, Shapiro DN, Saltman DL, Look AT. Fusion of a kinase

- gene, ALK, to a nucleolar protein gene, NPM, in non-Hodgkin's lymphoma. *Science*. 1994; 263: 1281-1284.
5. Bischof D, Pulford K, Mason DY, Morris SW. Role of nucleophosmin (NPM) portion of non-Hodgkin's lymphoma-associated NPM-anaplastic lymphoma kinase fusion protein in oncogenesis. *Mol Cell Biol*. 1997; 17: 2312-2325.
  6. Reiter A, Schrappe M, Tiemann M, Parwaresch R, Zimmermann M, Yakisan E, Dopfer R, Bucsky P, Mann G, Gander H, Riehm H. Successful treatment strategy for Ki-1 anaplastic large-cell lymphoma of childhood: a prospective analysis of 62 patients enrolled in three consecutive Berlin-Frankfurt-Munster group studies. *J Clin Oncol*. 1994; 12: 899-908.
  7. Brugieres L, Deley MC, Pacquement H, Meguerian-Bedoyan Z, Terrier-Lacombe MJ, Robert A, Pondarré C, Leverager G, Devalck C, Rodary C, Delsol G, Hartmann O. CD30+ anaplastic large-cell lymphoma in children: analysis of 82 patients enrolled in two consecutive studies of the French Society of Pediatric Oncology. *Blood*. 1998; 92: 3591-3598.
  8. Brugieres L, Quartier P, Le Deley MC, Pacquement H, Perel Y, Bergeron C, Schmitt C, Landmann J, Patte C, Terrier-Lacombe MJ, Delsol G, Hartman O. Relapses of childhood anaplastic large-cell lymphoma: treatment results in a series of 41 children--a report from the French Society of Pediatric Oncology. *Ann Oncol*. 2000; 11: 53-58.
  9. Seidemann K, Tiemann M, Schrappe M, Yakisan E, Simonitsch I, Janka-Schaub G, Dörffel W, Zimmermann M, Mann G, Gadner H, Parwaresch R, Riehm H, Reiter A. Short-pulse B-non-Hodgkin lymphoma-type chemotherapy is efficacious treatment for pediatric anaplastic large cell lymphoma: a report of the Berlin-Frankfurt-Munster Group Trial NHL-BFM 90. *Blood*. 2001; 97: 3699-3706.
  10. Lowe EJ, Sposto R, Perkins SL, Gross TG, Finlay J, Zwick D, Abromowitch M, Children's Cancer Group Study 5941. Intensive chemotherapy for systemic anaplastic large cell lymphoma in children and adolescents: final results of Children's Cancer Group Study 5941. *Pediatr Blood Cancer*. 2009; 52: 335-339.
  11. Woessmann W, Zimmermann M, Lenhard M, Burkhardt B, Rossig C, Kremens B, Lang P, Attarbaschi A, Mann G, Oschlies I, Klapper W, Reiter A. Relapsed or refractory anaplastic large-cell lymphoma in children and adolescents after Berlin-Frankfurt-Muenster (BFM)-type first-line therapy: a BFM-group study. *J Clin Oncol*. 2011; 29: 3065-3071.
  12. Le Deley MC, Reiter A, Williams D, Delsol G, Oschlies I, McCarthy K, Zimmermann M, Ruggières L, European Intergroup for Childhood Non-Hodgkin Lymphoma. Prognostic factors in childhood anaplastic large cell lymphoma: results of a large European intergroup study. *Blood*. 2008; 111: 1560-1566.
  13. Schmitz N, Trumper L, Ziepert M, Nickelsen M, Ho AD, Metzner B, Peter N, Loeffler M, Rosenwald A, Pfreundschuh M. Treatment and prognosis of mature T-cell and NK-cell lymphoma: an analysis of patients with T-cell lymphoma treated in studies of the German High-Grade Non-Hodgkin Lymphoma Study Group. *Blood*. 2010; 116: 3418-3425.
  14. Wan W, Albom MS, Lu L, Quail MR, Becknell NC, Weinberg LR, Reddy DR, Holskin BP, Angeles TS, Underiner TL, Meyer SL, Hudkins RL, Dorsey BD, et al. Anaplastic lymphoma kinase activity is essential for the proliferation and survival of anaplastic large-cell lymphoma. *Blood*. 2006; 107: 1617-1623.
  15. Piva R, Chiarle R, Manazza AD, Taulli R, Simmons W, Ambrogio C, D'Escamard V, Pellegrino E, Ponzetto C, Palestro G, Inghirami G. Ablation of oncogenic ALK is a viable therapeutic approach for anaplastic large-cell lymphomas. *Blood*. 2006; 107: 689-697.
  16. Kwak EL, Bang YJ, Camidge DR, Shaw AT, Solomon B, Maki RG, Ou SH, Dezube BJ, Jänne PA, Costa DB, Varella-Garcia M, Kim WH, Lynch TJ, et al. Anaplastic lymphoma kinase inhibition in non-small-cell lung cancer. *N Engl J Med*. 2010; 363: 1693-1703.
  17. Butrynski JE, D'Adamo DR, Hornick JL, Dal Cin P, Antonescu CR, Jhanwar SC, Ladanyi M, Capelletti M, Rodig SJ, Ramaiya N, Kwak EL, Clark JW, Wilner KD, et al. Crizotinib in ALK-rearranged inflammatory myofibroblastic tumor. *N Engl J Med*. 2010; 363: 1727-1733.
  18. Carpenter EL, Mosse YP. Targeting ALK in neuroblastoma – preclinical and clinical advancements. *Nat Rev Clin Oncol*. 2012; 9: 391-399.
  19. Soda M, Choi YL, Enomoto M, Takada S, Yamashita Y, Ishikawa S, Fujiwara S, Watanabe H, Kurashina K, Hatanaka H, Bando M, Ohno S, Ishikawa Y, et al. Identification of the transforming EML4-ALK fusion gene in non-small-cell lung cancer. *Nature*. 2007; 448: 561-566.
  20. Mori M, Ueno Y, Konagai S, Fushiki H, Shimada I, Kondoh Y, Saito R, Mori K, Shindou N, Soga T, Sakagami H, Furutani T, Doihara H, et al. The selective anaplastic lymphoma receptor tyrosine kinase inhibitor ASP3026 induces tumor regression and prolongs survival in non-small cell lung cancer model mice. *Mol Cancer Ther*. 2014; 13: 329-340.
  21. Choi YL, Soda M, Yamashita Y, Ueno T, Takashima J, Nakajima T, Yatabe Y, Takeuchi K, Hamada T, Haruta H, Ishikawa Y, Kimura H, Mitsudomi T, et al. EML4-ALK mutations in lung cancer that confer resistance to ALK inhibitors. *N Engl J Med*. 2010; 363: 1734-1739.
  22. Katayama R, Khan TM, Benes C, Lifshits E, Ebi H, Rivera VM, Shakespeare WC, Iafrate AJ, Engelman JA, Shaw AT. Therapeutic strategies to overcome crizotinib resistance in non-small cell lung cancers harboring the fusion oncogene EML4-ALK. *Proc Natl Acad Sci USA*. 2011; 108: 7535-7540.
  23. Katayama R, Shaw AT, Khan TM, Mino-Kenudson M, Solomon BJ, Halmos B, Jessop NA, Wain JC, Yeo AT,

- Benes C, Drew L, Saeh JC, Crosby K, et al. Mechanisms of acquired crizotinib resistance in ALK-rearranged lung cancers. *Sci Transl Med*. 2012; 4: 120ra17.
24. Delsol G, Campo E, Gascoyne RD. ALK-positive large B-cell lymphoma. In: Swerdlow SH, Campo E, Harris NL, Jaffe ES, Pileri SA, Stein H, Thiele J, Vardiman JW, eds. WHO Classification of Tumours of Haematopoietic and Lymphoid Tissues. 4th Edition. Lyon, France, International Agency for Research on Cancer, 2008: 254-255.
  25. Patnaik A, LoRusso P, Ball HA, Bahceci E, Yuen G, Papadopoulos KP, Kittaneh M, Tolcher AW. Pharmacokinetics and safety of an oral ALK inhibitor, ASP3026, observed in a phase I dose escalation trial. *J Clin Oncol*. 2013; 31: Abstract 2602.
  26. Turturro F, First AY, Arnold MD, Seth P, Pulford K. Biochemical differences between SUDHL-1 and KARPAS 299 cells derived from t(2;5)-positive anaplastic large cell lymphoma are responsible for the different sensitivity to the antiproliferative effect of p27Kip1. *Oncogene*. 2001; 20: 4466-4475.
  27. Bai RY, Dieter P, Peschel C, Morris SW, Duyster J. Nucleophosmin-anaplastic lymphoma kinase of large-cell anaplastic lymphoma is a constitutively active tyrosine kinase that utilizes phospholipase C- to mediate its mitogenicity. *Mol Cell Biol*. 1998; 18: 6951-6961.
  28. Shi P, Lai R, Lin Q, Iqbal AS, Young LC, Kwak LW, Ford RJ, Amin HM. IGF-IR tyrosine kinase interacts with NPM-ALK oncogene to induce survival of T-cell ALK+ anaplastic large-cell lymphoma cells. *Blood*. 2009; 114: 360-370.
  29. Shi B, Vishwamitra D, Granda JG, Whitton T, Shi P, Amin HM. Molecular and functional characterizations of the association and interactions between nucleophosmin-anaplastic lymphoma kinase and type I insulin-like growth factor receptor. *Neoplasia*. 2013; 15: 669-683.
  30. Zamo A, Chiarle R, Piva R, Howes J, Fan Y, Chilosi M, Levy DE, Inghirami G. Anaplastic lymphoma kinase (ALK) activates Stat3 and protects hematopoietic cells from cell death. *Oncogene*. 2002; 21: 1038-1047.
  31. Amin HM, McDonnell TJ, Ma Y, Lin Q, Fujio Y, Kunisada K, Leventaki V, Das P, Rassidakis GZ, Cutler C, Medeiros LJ, Lai R. Selective inhibition of STAT3 induces apoptosis and G1 cell cycle arrest in ALK-positive anaplastic large cell lymphoma. *Oncogene*. 2004; 23: 5426-5434.
  32. Rassidakis GZ, Feretzaki M, Atwell C, Grammatikakis I, Lin Q, Lai R, Claret FX, Medeiros LJ, Amin HM. Inhibition of Akt increases p27Kip1 levels and induces cell cycle arrest in anaplastic large cell lymphoma. *Blood*. 2005; 105: 827-829.
  33. Vishwamitra D, Li Y, Wilson D, Manshouri R, Curry CV, Shi B, Tang XM, Sheehan AM, Wistuba II, Shi P, Amin HM. MicroRNA 96 is a post-transcriptional suppressor of anaplastic lymphoma kinase expression. *Am J Pathol*. 2012; 180: 1772-1780.
  34. Matsuyama H, Suzuki HI, Nishimori H, Noguchi M, Yao T, Komatsu N, Mano H, Sugimoto K, Miyazono K. miR-135b mediates NPM-ALK-driven oncogenicity and renders IL-17-producing immunophenotype to anaplastic large cell lymphoma. *Blood*. 2011; 118: 6881-6892.
  35. Li Z, Graf N, Herrmann K, Junger A, Aichler M, Feuchtinger A, Baumgart A, Walch A, Peschel C, Schwaiger M, Buck A, Keller U, Dechow T. FLT-PET is superior to FDG-PET for very early response prediction in NPM-ALK-positive lymphoma treated with targeted therapy. *Cancer Res*. 2012; 72: 5014-5024.
  36. Mussolin L, Damm-Welk C, Pillon M, Zimmermann M, Franceschetto G, Pulford K, Reiter A, Rosolen A, Woessmann W. Use of minimal disseminated disease and immunity to NPM-ALK antigen to stratify ALK-positive ALCL patients with different prognosis. *Leukemia*. 2013; 27: 416-422.
  37. Damm-Welk C, Mussolin L, Zimmermann M, Pillon M, Klapper W, Oschlies I, d'Amore ES, Reiter A, Woessmann W, Rosolen A. Early assessment of minimal residual disease identifies patients at very high relapse risk in NPM-ALK-positive anaplastic large-cell lymphoma. *Blood*. 2014; 123: 334-337.
  38. Iwama E, Okamoto I, Harada T, Takayama K, Nakanishi Y. Development of anaplastic lymphoma kinase (ALK) inhibitors and molecular diagnosis in ALK rearrangement-positive lung cancer. *Onco Targets Ther*. 2014; 7: 375-385.
  39. Marsilje TH, Pei W, Chen B, Lu W, Uno T, Jin Y, Jiang T, Kim S, Li N, Warmuth M, Sarkisova Y, Sun F, Steffy A, et al. Synthesis, structure-activity relationships, and in vivo efficacy of the novel potent and selective anaplastic lymphoma kinase (ALK) inhibitor 5-chloro-N2-(2-isopropoxy-5-methyl-4-(piperidin-4-yl)phenyl)-N4-(2-(isopropylsulfonyl)phenyl)pyrimidine-2,4-diamine (LDK378) currently in phase 1 and phase 2 clinical trials. *J Med Chem*. 2013; 56: 5675-5690.
  40. Doebele RC, Pilling AB, Aisner DL, Kutateladze TG, Le AT, Weickhardt AJ, Kondo KL, Linderman DJ, Heasley LE, Franklin WA, Varella-Garcia M, Camidge DR. Mechanisms of resistance to crizotinib in patients with ALK gene rearranged non-small cell lung cancer. *Clin Cancer Res*. 2012; 18: 1472-1482.
  41. Tanizaki J, Okamoto I, Okabe T, Sakai K, Tanaka K, Hayashi H, Kaneda H, Takezawa K, Kuwata K, Yamaguchi H, Hatashita E, Nishio K, Nakagawa K. Activation of HER family signaling as a mechanism of acquired resistance to ALK inhibitors in EML4-ALK-positive non-small cell lung cancer. *Clin Cancer Res*. 2012; 18: 6219-6226.
  42. Yamada T, Takeuchi S, Nakade J, Kita K, Nakagawa T, Nanjo S, Nakamura T, Matsumoto K, Soda M, Mano H, Uenaka T, Yano S. Paracrine receptor activation by microenvironment triggers bypass survival signals and ALK inhibitor resistance in EML4-ALK lung cancer cells. *Clin Cancer Res*. 2012; 18: 3592-3602.
  43. Huang D, Kim DW, Kostakis A, Deng S, Lira P, Ho SN,

- Lee NV, Vizcarra P, Cao JQ, Christensen JG, Kim TM, Sun JM, Ahn JS, et al. Multiplexed deep sequencing analysis of ALK kinase domain identifies resistance mutations in relapsed patients following crizotinib treatment. *Genomics*. 2013; 102: 157-162.
44. Sasaki T, Okuda K, Zheng W, Butrynski J, Capaelletti M, Wang L, Gray NS, Wilner K, Christensen JG, Demetri G, Shapiro GI, Rodig SJ, Eck MJ, et al. The neuroblastoma-associated F1174L ALK mutation causes resistance to an ALK kinase inhibitor in ALK-translocated cancers. *Cancer Res*. 2010; 70: 10038-10043.
  45. Bresler SC, Wood AC, Haglund EA, Courtright J, Belcastro LT, Plegaria JS, Cole K, Toporovskaya Y, Zhao H, Carpenter EL, Christensen JG, Maris JM, Lemmon MA, et al. Differential inhibitor sensitivity of anaplastic lymphoma kinase variants found in neuroblastoma. *Sci Transl Med*. 2011; 3: 108ra114.
  46. Ceccon M, Mologni L, Bisson W, Scapozza L, Gambacorti-Passerini C. Crizotinib-resistant NPM-ALK mutants confer differential sensitivity to unrelated Alk inhibitors. *Mol Cancer Res*. 2013; 11: 122-132.
  47. Gambacorti Passerini C, Farina F, Stasia A, Redaelli S, Ceccon M, Mologni L, Messa C, Guerra L, Giudici G, Sala E, Mussolin L, Deeren D, King MH, et al. Crizotinib in advanced, chemoresistant anaplastic lymphoma kinase-positive lymphoma patients. *J Natl Cancer Inst*. 2014 Feb;106(2):djt378. doi: 10.1093/jnci/djt378
  48. Anastasov N, Klier M, Koch I, Angermeier D, Höfler H, Fend F, Quintanilla-Martinez L. Efficient shRNA delivery into B and T lymphoma cells using lentiviral vector-mediated transfer. *J Hematop*. 2009; 2: 9-19.
  49. Mohammad RM, Al-Katib A, Aboukameel A, Doerge DR, Sarkar F, Kucuk O. Genistein sensitizes diffuse large cell lymphoma to CHOP (cyclophosphamide, doxorubicin, vincristine, prednisone) chemotherapy. *Mol Cancer Ther*. 2003; 2: 1361-1368.
  50. Mori F, Ishida T, Ito A, Sato F, Masaki A, Narita T, Suzuki S, Yamada T, Takino H, Ri M, Kusumoto S, Komatsu H, Hishizawa M, et al. Antitumor effects of bevacizumab in a microenvironment-dependent human adult T-cell leukemia/lymphoma mouse model. *Eur J Haematol*. 2014; 92: 219-228.